Chapter

Study of the Parameters of the Planner with a Screw Working Body

Juraev Tojiddin Khayrullaevich,
Norov Sobirjon Negmurodovich
and Musulmanov Furqat Shodiyevich

Abstract

This chapter examined the theoretical background of the use of a screw working body in front of the planner bucket and conducting experiments in laboratory conditions with the proposed working body. This work supports the practical solution of using a screw working particle in the current field planning. Significance of the work reducing traction resistance to soil movement up to 20% enables the tractor unit to work at higher speeds of translational motion; the latter contributes to increased productivity, improved planning quality and reduced cash costs per unit of work performed. The chapter was prepared under results of research in the Mechanics Laboratory of Bukhara Engineering Technological Institute.

Keywords: productivity of the screw working body, translational speed of the planning unit, screw pitch, screw diameter, drawing prisms

1. Introduction

Further development of agriculture in modern conditions determines the introduction of new advanced technologies and machines for their implementation.

As we know, for increase of volume agricultural products, it is need to intensification of agricultural production, one of the means of which is wide land reclamation, which provides, as one of the most important measures, the planning of the irrigated land surface. Alignment of the surface of the fields by the long-base planners is of great importance in the range of planning works, and research work to improve these planners is carried out both in Uzbekistan and abroad.

The analysis of the state of the issue showed the need to improve the quality of planning work, increase the productivity of long-base planners and increase the levelling ability of the latter [1, 2].

2. Literature review

By world and domestic farming practices, it has been proved that planning or levelling the surface of the fields is the main land reclamation measure designed to eliminate irregularities on the field under sowing in the form of various rise and falls.

Many domestic and foreign scientific works [3–6] have been published on the need for field planning, authors of which have been examined the issue from different perspectives and pointed out the advantages of this operation. Moreover, there are many advantages, whether it is capital and operational planning or micro alignment. Experiments have established that under conditions of turbulent terrain, crop losses amount to 40% of the potential crop. Cotton grown on mounds and lowlands gives raw cotton of lower quality: fibre strength, grade, ripeness, etc. are reduced.

In areas with saline soil, a high-quality planning prevents the formation of saline spots (areas) and thereby ensures sustainable yields of all types of crops [6, 7]. Flushing saline lands without planning are ineffective.

According to Ref. [6], it was established that uniform soil moisture is achieved on the planned field, and the irrigation water consumption is significantly reduced.

In the United States, great importance is given to the planning of the surface of irrigated areas. Annually, in this country, approximately more than half of the irrigated areas are subject to planning [3, 6, 7]. Americans do not spare the cost of land planning, as this increases income from irrigated land and reduces the cost of production.

To ensure the high quality of the technological processes, including irrigation, it is necessary to pay special attention to the capital planning and the mandatory periodic implementation of the field operational planning.

3. Research methods

It is known that the magnitude and the nature of the change in the angular speed of a material particle determine the productivity and energy indicators for conveying the material with a screw [2, 8].

Let us consider the movement of a material particle of mass d_m located at point O of an inclined cylindrical screw at a distance *r* from the axis of the screw (**Figures 1** and **2**) and moving along the trajectory of the absolute movement AB; the axes *τ, b* and *n* are, respectively, tangent, binormal and normal to the trajectory of absolute motion [9]. The *n* axis is directed towards the centre of curvature and

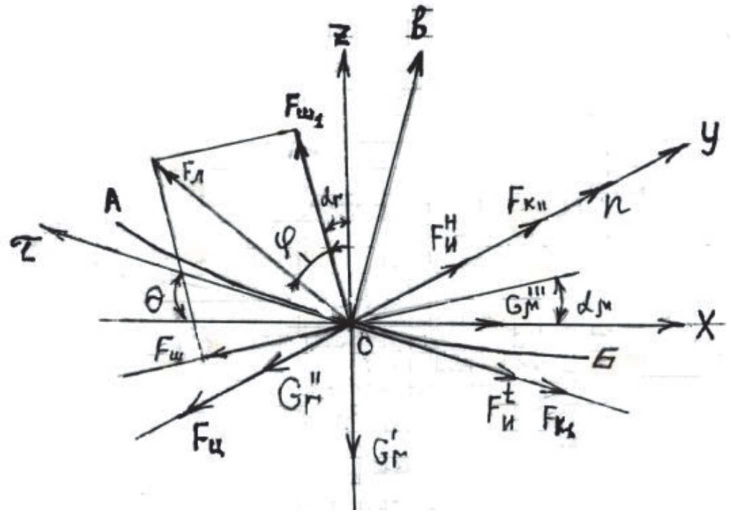

Figure 1.
Movement of a material particle of mass d_m located at point O.

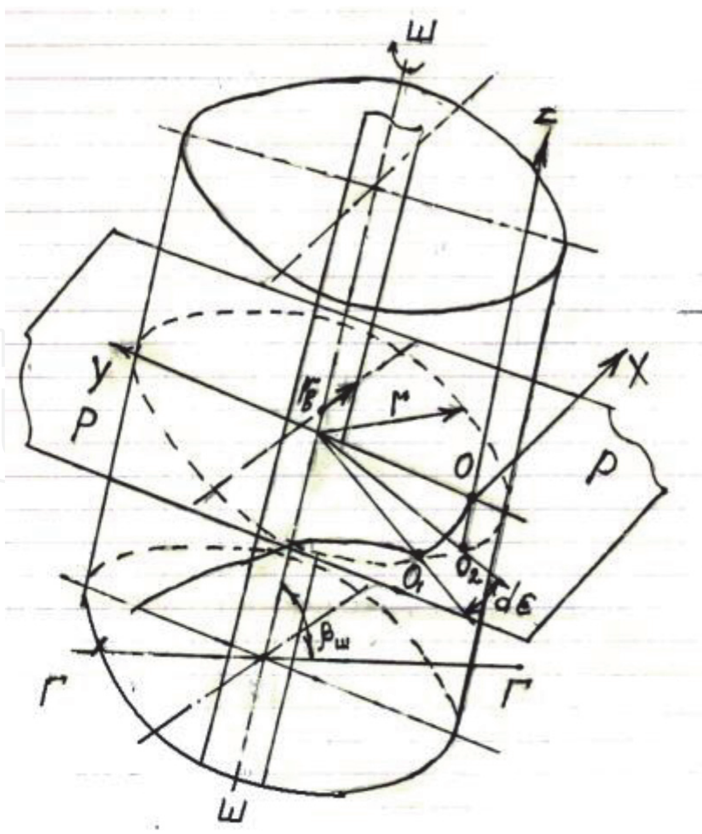

Figure 2.
Material particle of mass d_m located at point O of an inclined cylindrical screw at a distance r.

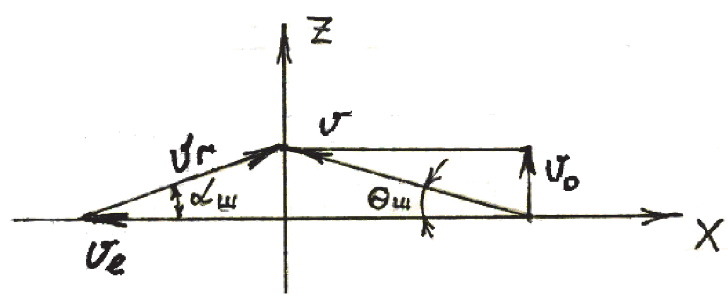

Figure 3.
Particle's absolute speed vector $\overline{V}$.

coincides with the y axis. The Z axis is parallel to the axis of the screw, and the x and y axes are located on tangent and normal in plane PP of the screw, perpendicular to its axis ШШ; GG horizontal plane.

The following forces impact on the soil particle: particle gravity Gr = gdm, which can be divided into three components, axial Gr^{I} = Gr.sin $\beta_{ш}$ (along the z axis), radial G_r^{II} = G_r.cos $\beta_{ш}$ cosε (along the y axis) and tangent G_r^{III} = G_r.cos$\beta_{ш}$·sinε (along the x axis); centrifugal force $F_ц = \omega_r{}^2 \cdot \mu \cdot d \cdot m$ (along the y axis), friction force of a particle on a blade casing F_{k_1} (along the τ axis), and friction force on a helical surface $F_ш$ (at an angle of inclination of the helix α_r to the x axis); tangential inertial force, $F_u{}^t$, acting along the tangent to the trajectory of the absolute motion of the particle (τ axis) and directed opposite to the particle's absolute speed vector $\overline{V}$ (**Figure 3**); normal inertial force directed to the centre of curvature of the trajectory (along the n axis); and normal reaction of the adjacent layer $F_{к_{II}}$ (along the n axis) and the helical surface $F_{ш_I}$ (at an angle a_r to the z axis). $\beta_ш$ is the angle of inclination of the screw to the horizon; and ε is the current angle of rotation of the particle, measured from the projection of the O_2 particle on the PP plane. The resultant $F_л$ of the normal reaction of the helical surface $F_{Ш_I}$ and the friction force against the helical surface $F_{ш} = fF_{ш_1}$ is deviated from the normal and the helical surface by the angle of friction $\phi = arctgf$, where *f* is the coefficient of friction of the soil over the screw metal. If we consider that the loosened soil before the bucket of the planner is clay, then the value of this coefficient is 0.6 ... 0.7. [8]

The friction force of a particle on a bucket caused by the combined action of forces $F_ц$ and G^{II}_r is equal to:

$$F_{k_1} = f_r\left(F_ц + G_r^{II}\right) = f_r\left(\omega_r^2 \cdot r + g\cos\beta_ш \cdot \cos\varepsilon\right) \cdot dm,$$

where f_r and *f*, respectively, are the friction coefficients of the particle on the bucket and the adjacent layer of material and the helical surface.

Absolute particle speed:

$$\vartheta = \sqrt{\vartheta_t^2 + \vartheta_o^2} = r\sqrt{\omega_r^2 + (\omega - \omega_r)^2 \cdot tg^2 a_r} \tag{1}$$

where ϑ_t is tangential particle speed at the radius *r* from the axis of the screw, $\vartheta_t = \omega_r \cdot r$; ϑ_o is the axial speed of the particle at a radius *r* from the axis of the screw, $\vartheta_o = (\omega \cdot \omega_r)tga_r$; ω is screw angular speed; and a_r is the angle of inclination of the helix of the screw on the radius *r* (**Figure 2**).

The tangent force of inertia is defined as follows:

$$F_u^t = \frac{d\vartheta}{dt}dm = \frac{r[\omega_r - (\omega - \omega_r)tg^2 a_r]}{\sqrt{\omega_r^2 + (\omega - \omega_r)^2 tg^2 a_r}} \cdot \frac{d\omega_r}{dt}dm \tag{2}$$

Normal inertial force:

$$F_u^н = \vartheta^2 \cdot r_a^{-1} \cdot dm = r^2\left[\omega_r^2 + (\omega - \omega_r)^2 \cdot tg^2 a_r\right] \cdot \left[r\left(1 + tg^2\theta\right)\right]^{-1}, \tag{3}$$

where r_a is the radius of curvature of the trajectory at the selected point, $r_a = r(1 + tg^2\theta)$; and θ is the angle of inclination of the helix of the particle trajectory to the axis X (**Figure 2**)

$$tg\theta = tga_ш(\omega - \omega_r)\omega_r^{-1}, \tag{4}$$

where $a_ш$ is screw helix angle at the periphery.

According to the D'Alembert's principle [8], the equation of dynamic equilibrium of a material particle in the projections on the axis of the natural trihedral of the trajectory (τ, b, n)(**Figure 2**) will be

$$\begin{aligned}\sum\tau = {}&\left[F_л\sin\left(a_r + \theta + \phi\right) - G_r^{III}\cos\theta - F_{k_1} - F_u^t - G_r^1\sin\theta\right] \cdot \cos\varepsilon -\\ &-\left(F_ц + G_r^{II} - F_u^H - F_{k^{II}}\right) \cdot \sin\varepsilon = O,\end{aligned} \tag{5}$$

$$\sum b = \pm F_л \cdot cos(a_r + \theta - \phi) + G_r^{III} \cdot \sin\theta - G_r^1 \cdot \cos\theta = 0, \tag{6}$$

$$\begin{aligned}\sum n = {}&\left(F_ц + G_r^{II} + F_u^H - F_{k_{ii}}\right) \cdot \cos\varepsilon + \left[F_л\sin\left(a_r + \theta + \phi\right) -\right.\\ &\left.-G_r^{III} \cdot \cos\theta - F_{k1} - F_u^t - G_r^1\sin\theta\right] \cdot \sin\varepsilon\end{aligned} \tag{7}$$

Solving these equations jointly, excluding the force $F_л$ from them, after the corresponding transformation of the exception and time by expressing the elementary angle of rotation along the arc O_1, O_2 (**Figure 1**) of the particle $d\varepsilon = (\omega - \omega_r)dt$, we obtain:

$$\frac{d\omega_r}{d\varepsilon} = \frac{\pm\dfrac{sin([a_r + \phi)\omega_r + \cos(a_r + \phi)\cdot tga_r(\omega - \omega_r)}{\cos(a_r + \phi)\omega_r - \sin(a_r + \phi)tga_r(\omega - \omega_r)}}{(\omega - \omega_r)r[\omega_r - (\omega - \omega_r)tg^2 a_r]} \rightarrow$$
$$\rightarrow \frac{[g\cdot\sin\beta_{ш}\cdot\omega_r - g\cdot\cos\beta_{ш}\sin\varepsilon\cdot tga_r(\omega - \omega_r)] -}{(\omega - \omega_r)r[\omega_r - (\omega - \omega_r)tg^2 a_r]} \rightarrow$$
$$\rightarrow \frac{-f_r(\omega_r{}^2 + g\cdot\cos\beta_{ш}\cdot\cos\varepsilon)x\sqrt{\omega_r{}^2 + (\omega - \omega_r)^2\cdot tg^2 a_r} -}{(\omega - \omega_r)r[\omega_r - (\omega - \omega_r)tg^2 a_r]} \rightarrow \tag{8}$$
$$\rightarrow \frac{-g\cdot\sin\beta_{ш}\cdot tga_r(\omega - \omega_r) - g\cdot\cos\beta_{ш}\sin\varepsilon\cdot\omega_r}{(\omega - \omega_r)r[\omega_r - (\omega - \omega_r)tg^2 a_r]}$$

By integrating Eq. (8) by the Euler method [3], we can obtain the curves of the dependence of ω_r on ε for screws with different parameters.

In the inclined screw, there is a periodically steady motion of the material particle. The maximum value of $\omega_r{}^{max}$ is on the plot with the values of the angle $2k\pi > \varepsilon > (2k-1)\pi$, and the value of $\omega_r{}^{min}$ is in the zone $(2k+1)\pi > \varepsilon > 2k\pi$, where (k) is any number. In order to simplification for inclined screws, it is possible to take the average value of the angular speed in the area of periodically steady motion:

$$\omega_r{}^{cp} = \int_{\varepsilon=2k\pi}^{\varepsilon=(2k+1)\pi} \cdot\omega_r d\varepsilon \cong \frac{\omega_r{}^{2k\pi} + \omega_r{}^{(2k+1)\pi}}{2} \tag{9}$$

The values of $\omega_r{}^{max}$ and $\omega_r{}^{min}$ can be found by progressive approximation from Eq. (8), equating the right side to zero at $\varepsilon = 2k\pi$ and $\varepsilon = (2k+1)\pi$. However, for practical purposes, the angular speed of a soil particle at the periphery of the screw can be taken as:

$$\text{for vertical screws, } 0,4\,\omega < \omega_{r_ш} < 0,5\omega,$$
$$\text{for steeply inclined screws, } (\beta_ш \geq 30^o)\ 0,3\omega < \omega_{r_ш} < 0,4\omega,$$

where $\omega_{r_ш}$ is the particle angular speed at the periphery of the screw, sec^{-1}.

The study of Eq. (8) showed that in a certain zone limited by the cylindrical contour of the soil shaft, soil particles relatively quickly acquire the angular speed of the screw and their lifting stops [8]. The value of the so-called critical radius $r_{кр}$ depends on the initial conditions and is determined from Eq. (8) after substituting $\omega_r = \omega$ at $d\omega_r/d\varepsilon = 0$.

In the horizontal $(\beta_ш < 30°)$ screw, during the period of steady motion, the angular speed of the particle is zero. The angle of rotation of the particle ε, at which the steady motion begins, depends on the initial conditions and can be found from Eq. (8):

$$\varepsilon = arctg\left[f_r \sin(a_r + \phi)\cos^{-1}(a_r + \phi)\right] \tag{10}$$

Maximum productivity on loosened soil, determined by the throughput between the upper turns of the screw will be:

$$\Pi = \int_{r_{кр}}^{r_{ш}} \vartheta_r dS, \tag{11}$$

where $r_{ш}$ is the outer radius of the screw; ϑ_r is the ground sliding speed on the helical surface of the screw (relative speed); and dS is the elementary cross-sectional area of the soil located between the upper turns in a plane perpendicular to the relative speed vector.

The screw capacity in a dense body will be:

$$\Pi_T = \frac{1}{K_p} \int_{\kappa_{кр}}^{r_{ш}} \vartheta_r \cdot dS^I, \tag{12}$$

where κ_p is soil loosening coefficient; for our case, κ_p = 1.14 ... 1.28 [8].

Soil in the cross section of the screw by a plane, passing through the axis of the screw, occupies an area bounded from below by a straight-line perpendicular to the axis of the screw (**Figure 4**). Then in the cross section, we get a rectangle of length l^{II}, which can be taken equal to the pitch of the screw $l^{II} = l^{I}_{ш}$.

The elementary area of soil cross-section at a distance r from the screw axis will be equal to:

$$dS = dS_1 \cdot \cos a_r = l^1{}_{ш} d_r \cos a_r = 2\pi l^1{}_{ш} \left(\sqrt{4\pi^2 \cdot r^2 + \left(l^1{}_{ш}\right)^2} \right)^{-1} \cdot r d_r, \tag{13}$$

where dS_1 is the elementary area of soil in axial cross-section (**Figure 4**).

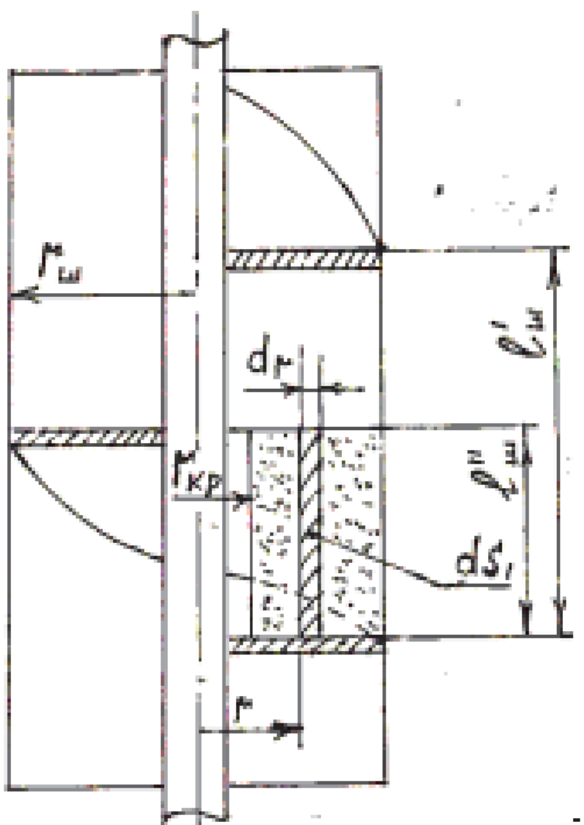

Figure 4.
Position of soil area in the cross section of the screw.

In horizontal and gently dipping screws at inclination angle $\beta_ш \leq 30°$, the angular speed of the material particle is $\omega^{cp}{}_{r_ш} = 0$. To calculate the capacity (m^3/h), we can use [1] the following formula:

$$П_T = 450\left(d_ш{}^2 - d_b{}^2\right)l_ш{}^1\omega \cdot K_H K_\beta \cdot K_p{}^{-1}, \tag{14}$$

where $d_ш$, $d_в$, respectively, are the diameters of the screw and shaft, m; $K_н$ is the screw filling coefficient, for our case we can take equal to $K_н = 0,2\ \dots\ 0,4$; and K_β is the coefficient taking into account the angle of inclination of the screw to the horizon $\beta_ш$, $K_\beta = 1,0 \dots 0,8$ [8].

3.1 Selection and justification of the main parameters of the screw

The main parameters of working elements of the screw include the length of the conveying part—$l_ш$, the length of the cutting part—l_p, the diameter of the screw—$d_ш$, peripheral speed on the cutting edge—$\vartheta_{окр}$, the pitch of the screw—$l^1{}_ш$ and the working speed of movement—ϑ_p.

The length of the conveying and cutting parts of the screw is taken constructively, based on the type of screw and the parameters of the medium being processed. For preliminary calculations, we can take the length of the conveying part of the horizontally located screw $l_ш = l_p = (0,7 \dots 0,8)\ в_n$, where $в_{\text{n}}$ is the width of the planner scoop.

The diameter of the screw $d_ш$ with a horizontal working body at the given productivity $П_т{}^1 = П_т$ can be determined from formula (14) after some transformations, m;

$$d_ш \geq \sqrt{П_T{}^1 \cdot K_p\left(900\vartheta_{окр} \cdot K_a K_н \cdot K_\beta\right)^{-1} + d^2{}_в}, \tag{15}$$

where $\vartheta_{\text{окр}}$ is the peripheral speed on the cutting edge of the screw, $\vartheta_{\text{окр}} = 1.5 \dots 3$ m/sec; and K_a is the coefficient taking into account the inclination of the cutting edge of the screw, $K_a = l^1{}_ш/d_ш = 0,7 \dots 1,0$. Other designations see from the formula (14).

The step of the horizontal screw $l^1{}_ш$ is taken equal to $l^1{}_ш = K_a d_ш$, the value of K_a is taken depending on the inclination of the cutting edge of the screw. For our case, we can take K_a equal to 0.85.

The working speed of the soil movement with the screw should be equal to the speed of filling the planner bucket with soil. The latter depends on the forward speed of movement of the planner. For our case, with a certain accuracy, we can take $\vartheta_{гр} = \vartheta_{ков} = \vartheta_{\text{п}}$, where $\vartheta_{гр}$ is the speed of the soil movement with the screw, $\vartheta_{ков}$ is the speed of filling the planner bucket with soil and $\vartheta_{\text{п}}$ is the forward speed of the planner, m/s.

The working speed of the planner's movement can also be determined from the conditions for ensuring a given efficiency on a cut of soil with the planner's bucket. For a horizontal screw, operating speed ($\vartheta_{\text{п}}$) of movement is (m/s):

$$\vartheta_П = П_T \cdot l_p{}^{-1} \cdot h_p{}^{-1}, \tag{16}$$

where $П_т$ is the efficiency of the planning unit on cut of soil, m^3/sec; l_{p} is the cutting length of the planner's knife, m; and h_{p} is the thickness of the cut soil layer, m.

Based on the analysis of the above theoretical background in the determination of the efficiency of the screw working body, it is suggested that with the increase in the speed of rotation and in diameters of the screw, the productivity of the screw working body increases. The screw pitch is also of great importance, with an increase in which the volume of soil moved to the sidewalls of the planner bucket increases, which in turn contributes to an even distribution of the soil of the drawing prism along the width of the planner passage. With an increase in the speed of forward movement of the planner increases the working capacity of the screw working body, that is screws move a large volume of soil to the sides relative to each other. However, such an improvement in the work of working element of the screw for our case, as shown by selective experiments with the experimental sample of a mini-planner, occurs up to a speed of 2 m/s of the forward movement of the unit. Above this speed, the screws begin to become clogged with soil, and the technological process of the screw working body is violated.

We derived the equation of traction resistance of the planner, which has the following form:

$$P = f_n G_n + \frac{\left[\sin\beta\left(1-f^2\right)2f\cos\beta\right]\tau\cdot S}{\sin\left(\beta+\theta\right)\left(1-\mu f\right)+\cos\left(\beta+\theta\right)\left(\mu+f\right)} + \frac{1}{3}\lambda_v l^3 tg^2\varphi_0 tg^2\left(45-\frac{\beta}{2}\right)f + $$
$$+G_{np}\left(f\cos^2\beta + tg\rho + \frac{2V^2\sin^2\frac{\beta}{2}}{Kycm\cdot g}\right) \tag{17}$$

where f_n- planner rolling resistance coefficient; G_n- mass of the planner; $\beta-$ cutting angle; $f, \mu-$ coefficients of friction of soil on steel and soil on soil; $\tau-$ shear stress; $S-$ shear area; $\theta-$ shear angle; λ_v- volumetric mass of soil as in the function of movement speed; $l-$ bucket side length; φ_0- angle of slope of the soil roller during movement; $G_{np}-$ mass of the soil roller; $V-$ unit movement speed; and $Kycm-$ coefficient taking into account the design of the rear wall of the bucket [10].

4. Results and discussion

From the analysis and conclusions we can see that with the increase in the rotation speed and diameter of the screw, the productivity of the screw working element increases. The screw pitch is also of great importance, with an increase in which increases the amount of soil movement to the sidewalls of the planner bucket, which in turn contributes to uniform distribution of the soil of the drawing prism along the width of the planner. With the increase in the speed of translational movement of the planner increases the functionality of the screw working element, that is the screws move a large volume of soil to the sides relative to each other. Below in **Figure 5**, the location of the screws in the bucket of the planner is shown.

However, such improvement in the work of the screw working element for our case, as shown by selective experiments with the experimental sample of a mini-planner, occurs up to the speed of 2 m/s of translational movement of the unit. Above this speed, the screws begin to be clogged with soil, and the technological process of the screw working body is violated. Below in **Figure 6**, experimental sample of a mini-planner with a screw working body is shown.

The above analysis requires investigating the productivity of the screw working body, depending on the rotation speed, diameter and pitch of the screw. Therein, the translational speed of the planning unit is also of significant importance. Because, the volume of the planner's bucket filled with soil per unit of time should be equal to the volume of the processed soil by the screws.

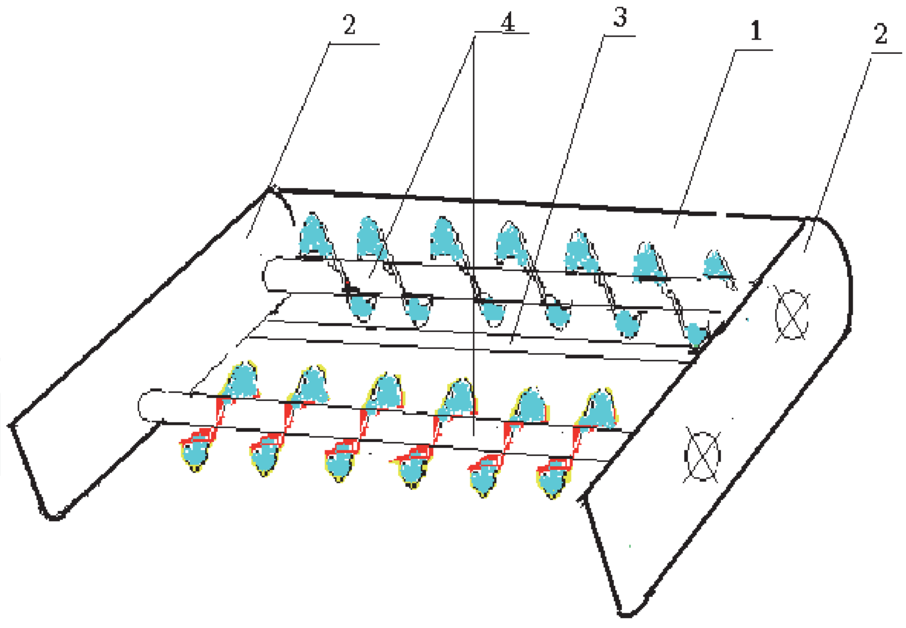

Figure 5.
Scheme of the location of the screws in the bucket of the planner (1—rear wall of the bucket, 2—tank walls, 3—knife of the rear wall and 4—screws).

Figure 6.
General view of the experimental prototype of the mini planner.

Below are the curves (**Figures 7–9**) of the change in productivity of the screw working element of the planner depending on the rotation speed, diameter and pitch of the screw.

As we can see from the graph (**Figure 7**), with the increase in screw rotation, the screw productivity is directly proportional to screw rotation. At a screw rotation of 40 rpm, the screw capacity is 2.56 m^3/h, and at screw rotation of 240 rpm, the screw capacity increases to 15.38 m^3/h. That is, the productivity of the screw increases by six times. This increase in productivity approximately corresponds to the desired performance of the planning unit.

The change in the performance of the screw in the function (D_s) of the diameter of the screw is shown in **Figure 8**.

Analysing this graph, we can say that the change in productivity along its diameter has curvilinear nature. Moreover, part of the curve to the point corresponding to D_s = 180 mm is a power-law nature, and then the curve changes linearly. Further increase in the diameter of the screw (D_s) leads to the increase in its productivity so that the planner will not be able to provide the screws with soil for their normal operation. In addition, the increase in the given productivity of the

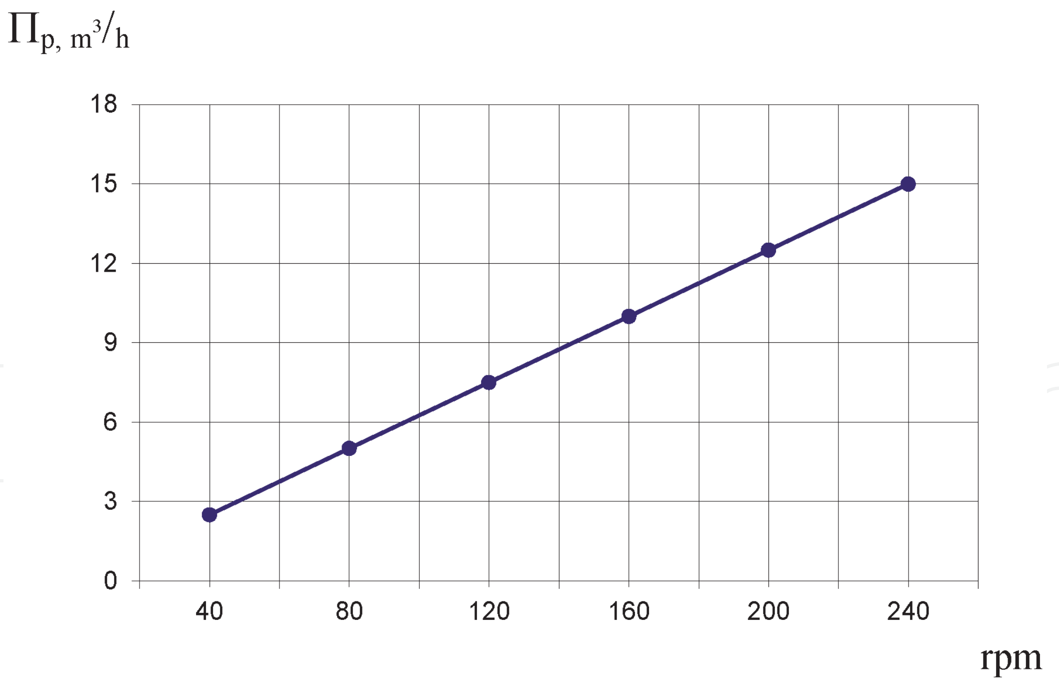

Figure 7.
Change of the productivity of the screw working element depending on the speed of rotation of the screws (at D_p = 0.18 m, S_p = 0.15 m and $K_н$ = 0.28—bucket filling ratio).

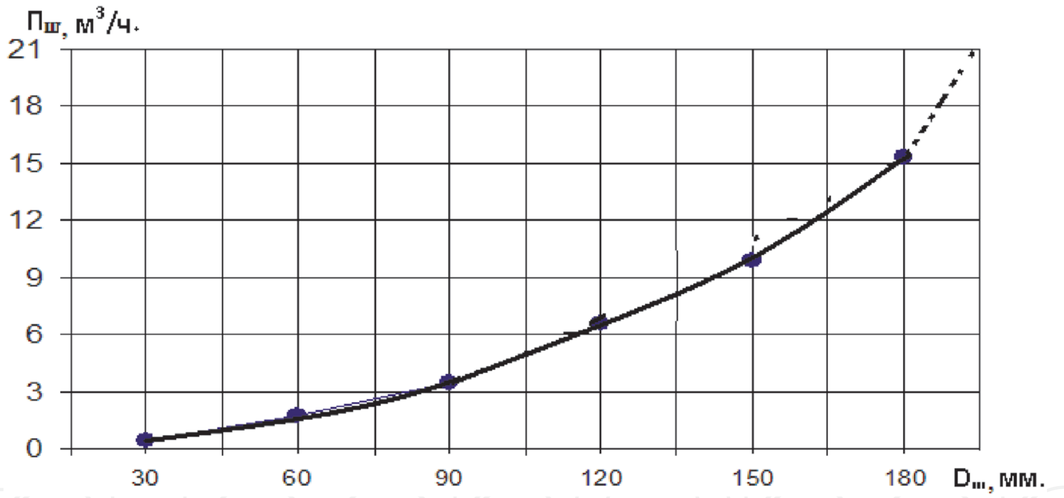

Figure 8.
Change in productivity of the screw working element depending on the diameter (Ds) of the screw (at S_s = 0.15 m, n_s = 240 rpm and $K_н$ = 0.28).

scheduler, which is accompanied by the increase in the translational speed of the movement of the unit above 7.5 km/h, leads to a disruption of the technological process of planning and the decrease in the quality indicators of field levelness [3].

The graph of the performance of the screw working element depending on the pitch (S_m) of the screw is shown in **Figure 9**.

As we can see from the graph, with the increase in the pitch of the screw (S_s), its productivity changes in direct proportion to the changes in the pitch (S_s), that is the functional change in the curve is linear. If with a screw pitch of 30 mm, the screw capacity is 3.07 m^3/h, then with a screw pitch of 180 mm, the productivity increases to 18.45 m^3/h, that is it increases six times.

Analysis of the graph (**Figure 9**) shows that increasing the screw pitch to 180 mm increases the capacity to 18.45 m^3/h, which is almost to 3 m^3 more than at the screw pitch S_s = 150 mm. Such an increase in the productivity of the screw

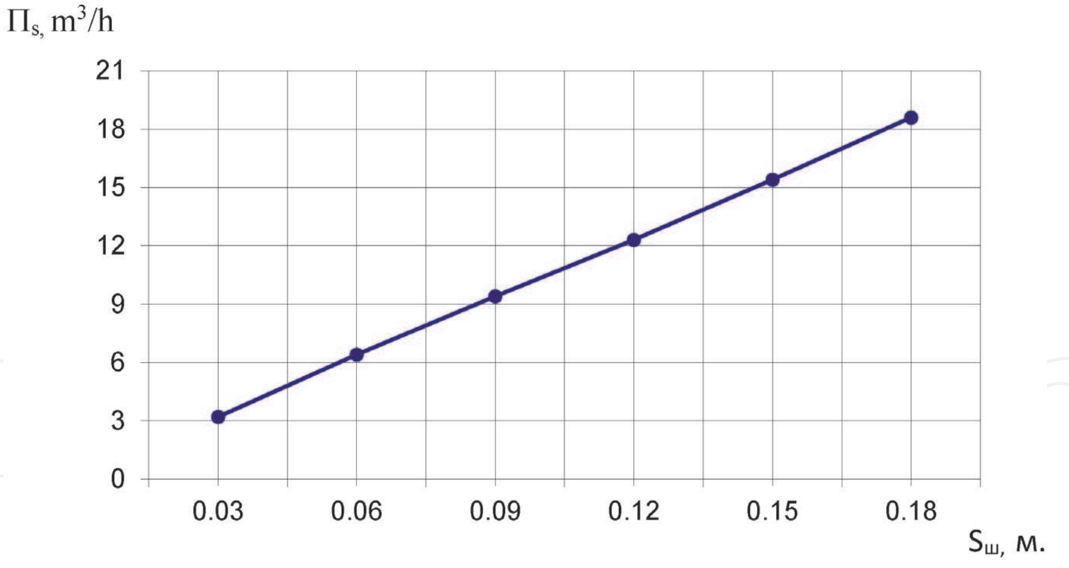

Figure 9.
Change in the productivity of the screw working element depending on the pitch (S_s) of the screw (at D_s = 0.18 m, n_s = 240 rpm and $K_н$ = 0.28).

working element could be obtained with a further increase in its diameter (D_s). But it is known that the increase in the diameter (D_s) of the screw is accompanied by greater energy consumption during its operation compared to the increase in the pitch of the screw. Therefore, a theoretical study of the work of the screw working element in the bucket of the planner allows us to conclude that for a given productivity of the planning unit, it is advantageous and advisable to use the screw parameters: D_s = 180 mm, n_s = 240 rpm and screw pitch S_s = 180 mm.

Increase in the productivity of the screw working element due to the increase in the pitch of the screw reduces the metal consumption of the screw and the corresponding material costs in comparison with the increase in the diameter (D_s) of the screw. In addition, further increase in the diameter of the screw causes difficulties in their layout in the bucket of the planner.

Using the methodology for conducting scientific research and processing the obtained data [2, 10], we derived empirical equations (formulas) of dependencies $y = f(n_ш)$, $y = f(D_ш)$ and $y = f(S_ш)$. For the graphs of **Figures 7–9**, respectively, $y_1 = 0,064X$; $y_2 = 474,7X^2$; and $y_3 = 102,5X$, the curve of which is consistent with the curves shown in **Figures 7–9**.

The screw working body surface was geometrically modelled by corresponding author and the offered geometric models give possibility to control engineering and technological parameters by optimization of geometric parameters of working surface, which may use this possibility in designing the working body of screw planners through exporting CAD models to CAE system [9, 11–15].

Author details

Juraev Tojiddin Khayrullaevich[1]*, Norov Sobirjon Negmurodovich[2] and Musulmanov Furqat Shodiyevich[1]

1 Tashkent Institute of Irrigation and Agriculture Mechanization Engineers, Bukhara Branch, Uzbekistan

2 Bukhara Engineering-Technological Institute, Uzbekistan

*Address all correspondence to: tojiddin_1968@mail.ru

References

[1] Khasanov IS, Norov SN. Theoretical background of the results of experiments on the use of screw before the planner bucket. Universum: Technical Sciences Moscow. 2019;**12** (69):41–44

[2] Norov SN, Hamraeva MF. Analytical research of determining the maximum efficiency of planning machines. International Journal of Advanced Research in Science, Engineering and Technology. 2019:**6**(6):361-362. Available from: http://www.ijarset.com/upload/2019/june/37-IJARSET-Abrorov-51.pdf

[3] Norov SN. Research and Development of a Machine System for Complex Mechanization of Precultival Treatment of Agricultural Conditions in the Bukhara Region. Deutschland, Germany: LAP LAMBERT Academic Publishing; 2019. p. 65. Available from: https://www.lap-publishing.com/

[4] Efremov AN. Laser Planning of Irrigated Lands. Moscow. 2016. Available from: https://www.ya-fermer.ru/sites/default/files/lasernayaplanirovka_0.pdf

[5] Antonov EV. Development of technological process of planning rice drafts using the multifunctional planning machine [Dissertation for the degree of candidate of technical sciences]. Russia. 2008

[6] Efremov AN, Yu NS. Machines and technologies of capital planning of rice drafts. Tractors and Agricultural Machinery. 2016;**3**:37

[7] Efremov AN. The method of calculating the operational efficiency of levers. Construction and Road Machines. 2015;**5**:42-46

[8] Khasanov IS, Norov SN. Theoretical background for determining some parameters of the screw working jointly with the planner bucket. Agrarian Science Journal, Moscow, 2015;**6**

[9] Juraev TK. Design the working surface based on the particle trajectory. In: Proceeding Outs of Conference “AVIA-2013”. Kiev: NAU; 2013. pp. 21–23. Available from: https://scholar.google.com/scholar?cluster=7986884450713291378&hl=en&oi=scholarr

[10] Norov SN. Theoretical background for research of tractive effort of the planner. In: Collected papers of XXII International Scientific-Practical conference “Russian Science in the Modern World”. Moscow. 2019. Available from: http://xn–80aa3afkgvdfe5he.xn–p1ai/RNSM-22_originalmaket_N-1.pdf

[11] Juraev TK. Decision maintenance management problems in agriculture Engineering by Constructive Geometric Modeling Methods. Maintenance Management. Edited by Fausto Pedro García Márquez and Mayorkinos Papaelias. London, United Kingdom. 2020. pp. 23-37. https://mts.intechopen.com/storage/books/8623/authors_book/.

[12] Juraev T.Kh, Murodov N.M, Naimov S.T. Application the Geometric Modeling Methods and Systems in Design Engineering and Manufacturing on Example of Agriculture Engineering. /Design and Manufacturing. /Edited by Evren Yasa, Mohsen Mhadhbi and Eleonora Santecchia. First published in London, United Kingdom, 2020 by IntechOpen, 211-231 p. http://dx.doi.org/10.5772/intechopen.83290.

[13] Juraev TK. Creating the geometric database for product lifecycle management system in agricultural engineering. In: International Conference on Information Science and Communications Technologies ICISCT

2017 Applications, Trends and Opportunities; 2-4 November 2017, TUIT, Tashkent, Uzbekistan. IEEE Catalog Part Number: CFP17H74-CDR, ISBN: 978-1-5386-2167-7. 2017. Available from: https://www.researchgate.net/publication/321821311

[14] Juraev TK. Conceptual design of moldboard based on geometric modeling. In: Theory and Application of Design. Kiev: NAU; 2012. №. 1. pp. 75-81. Available from: http://www.irbis-nbuv.gov.ua/cgi-bin/irbis_nbuv/cgiirbis_64.exe?C21COM=2&I21DBN=UJRN&P21DBN=UJRN&IMAGE_FILE_DOWNLOAD=1&Image_file_name=PDF/tprd_2012_1_13.pdf

[15] Juraev TK. Modeling the directory curve of moldboard surface by conic. Applied Geometry and Engineering Graphic. Kiev: KNUCA; 2011. №. 87. Available from: https://scholar.google.com/scholar?cluster=2210113268218384828&hl=en&oi=scholarr